Japanese Journal of Veterinary Research 71(4): 121-129, 2023

JJVR

SHORT COMMUNICATION **Regional Study**

Ability of *Pasteurella canis* isolated from host animals and human patients in Japan to invade human keratinocytes: associations between cell invasion ability and host or genotypic traits

Haruno Yoshida[1)], Takahiro Maeda[1)], Mieko Goto[1)], Yuzo Tsuyuki[1,2)], Kenichi Shizuno[1,3)] and Takashi Takahashi[1,*)]

[1)] Laboratory of Infectious Diseases, Graduate School of Infection Control Sciences and Ōmura Satoshi Memorial Institute, Kitasato University, Tokyo, Japan
[2)] Division of Clinical Laboratory, Sanritsu Zelkova Veterinary Laboratory, Tokyo, Japan
[3)] Department of Clinical Laboratory, Chiba Kaihin Municipal Hospital, Chiba, Japan

Received for publication, September 25, 2023; accepted, November 15, 2023

Abstract

We examined human keratinocyte cell invasion ability (CIA) of *Pasteurella canis* from 17 animals and 13 humans with relationships between CIA and host/genotypic traits. We designated CIA higher than isolate mean as high-frequency and that lower than mean as low-frequency. Repetitive element-based fingerprinting dendrograms were constructed; virulence-associated genes were clustered in phylogenetic trees. High-frequency CIA was observed in 9 isolates; low-frequency CIA in 21. No relationships were observed between high-frequency CIA and host/source. Dendrograms showed no associations between high-frequency CIA/host and different clades (A–1/–2; B–1/–2/–3). Trees with *ptfA–ompA* alleles showed no associations between high-frequency CIA/host and different clusters (1/2; 1/2/3). Our observations suggest CIA assessment feasibility without relationships between high-frequency CIA and host/genotypic traits.

Key Words: Cell invasion ability, Human keratinocyte, *Pasteurella canis*

The pathogenesis of bacterial infections is initiated by the adhesion of bacteria to the host cells. Some microorganisms have evolved a specialized strategy to survive and escape host immune systems by entering host cells (referred to as "intracellular invasion" or "internalization")[4)]. These invasive bacteria are localized in membrane-bound phagosomes. Some microorganisms can evade the cytoplasm within a few hours of destroying the phagosome membrane, whereas others remain entrapped[5)]. Under the former conditions, pathogens can survive intracellularly, multiply, and eventually spread to adjacent cells; under the latter situations, phagosome fusion with vacuoles produces an intracellular degradation environment, resulting in bacterial lysis[5)]. We evaluated the cell invasion ability (CIA) of *Streptococcus agalactiae*[17)] and *S. canis*[16)] using human colon cancer epithelium and keratinocyte (HaCaT) cell lines.

* Corresponding author: Professor Takashi Takahashi, M.D., Ph.D.
Laboratory of Infectious Diseases, Graduate School of Infection Control Sciences and Ōmura Satoshi Memorial Institute, Kitasato University
5-9-1 Shirokane, Minato-ku, Tokyo 108-8641, Japan
Tel: +81-3-5791-6428, Fax: +81-3-5791-6441, E-mail: taka2si@lisci.kitasato-u.ac.jp
doi: 10.57494/jjvr.71.4_121

Pasteurella canis was previously classified as *Pasteurella multocida* biotype 6 and reclassified in 1985 based on DNA homology[10]. This bacterium is a tiny, non-motile, facultatively anaerobic, gram-negative coccobacillus belonging to a species of *Gammaproteobacteria* in the family *Pasteurellaceae*. *P. canis* forms smaller colonies compared to the larger ones of *P. multocida* when the isolates are inoculated onto sheep blood agar plates and incubated in 5% CO_2 at 37 °C for 24 hr[9], suggesting that *P. canis* has a relatively slower growth capacity than *P. multocida* under the same culture conditions. Phylogenetic trees showing the relationships between the 16S rRNA sequences and fragment sequences of the superoxide dismutase gene from the type strains of *Pasteurella* demonstrated that *P. canis* is more closely related to *P. stomatis* and *P. dagmatis* than *P. multocida*[4].

P. canis is a zoonotic pathogen mainly transmitted from animals to humans through animal bites or deep contact with animals. The Emergency Medicine Animal Bite Infection Study Group[15] conducted a bacteriological evaluation of infected wound sites resulting from dog and cat bites and showed that *P. canis* was the most common species isolated from wounds caused by dog bites, whereas *P. multocida* was the most common pathogen isolated from wounds caused by cat bites. Human skin and subcutaneous tissues are one of the main *P. canis* entry sites through animal bites.

Genotypic approaches, including repetitive element-based fingerprinting using randomly amplified polymorphic DNA-based polymerase chain reaction (RAPD-PCR)[1,11] and M13-based PCR[6], have been used to perform epidemiological analyses of *P. multocida* isolates. The RAPD-PCR consists of short oligonucleotide forward/reverse primers of the arbitrary sequences with 8–12 nucleotides, and the M13 (a single primer) PCR fingerprinting and similar techniques are successfully employed to different species, including *Porphyromonas*, *Bacteroides fragilis* group, *Leptospira*, *Staphylococcus*, and *Streptococcus*. Additionally, of the virulence-associated genes (VAGs), *tadD* (encoding tight adherence protein D)[2], *ptfA* (encoding type IV fimbriae)[12], and *ompA* (encoding outer membrane protein A)[7] were targeted for the molecular characterization of *P. multocida* isolates previously.

Basic investigations of *P. canis* isolates are scarce, especially studies on their virulence factors (including human keratinocyte entry ability) and genotypic traits. This study aimed to clarify the CIA of animal and human isolates from Japan. We determined the genotypic features of the isolates using RAPD-/M13-PCR fingerprinting data and VAG profiles containing *tadD–ptfA–ompA*. We also analyzed significant associations between CIA and host information or genotypic traits.

Thirty *P. canis* isolates from diseased dogs (n = 16), an ill cat, and human patients (n = 13) were analyzed (Table 1). Isolation years were 2017 (n = 4), 2018 (n = 2), 2019 (n = 11), 2021 (n = 11), and 1997/1998 (n = 1 for each). The isolation sources were pus/skin (n = 17), upper/lower respiratory tract (n = 11), and ear/blood (n = 1 for each). The prefectures included Chiba (n = 14), Tokyo (n = 8), Saitama (n = 3), and Kanagawa/Aichi/Gifu/Nagasaki/Okayama (n = 1 for each). One isolate per one host was stored at –70 °C to –80 °C in-hospital or in a commercial laboratory and was sent to our laboratory for further genotypic/phenotypic analyses processed.

DNA was extracted from the isolates by suspending them in Tris-EDTA buffer and boiling them at 97 °C for 10 min. *P. canis* identification was based on 16S rRNA sequences determined by PCR and direct sequencing.

Based on the similar growth curve data of three *P. canis* isolates (PA42/PA57/PA78), the expected bacterial count became 5×10^8 colony-forming units (CFU)/mL when the optic density at 600 nm revealed 1. CIA measurement using HaCaT cell lines was performed as previously described[16,17], with the following modifications: the multiplicity of infection used was 100 for mid-log growth phase *P. canis* based on the bacterial count; isolates resuspended in Dulbecco's modified Eagle's medium (DMEM) were added to semiconfluent HaCaT cells ($2–5 \times 10^5$ cells/well) and grown in a 12-well culture plate with

Table 1. Backgrounds, cell invasion ability (CIA), and genotypic features of thirty *P. canis* isolates.

Isolate no.	Host species	Sex	Age (year-old)	Isolation year	Isolation source	Prefecture	CIA CFU /100 cells	CIA frequency	RAPD fingerprinting	M13 fingerprinting	Virulence-associated gene profile		
							mean ± SD	High/low	clade	clade	*tadD*	*ptfA* (GenBank accession no.)	*ompA* (GenBank accession no.)
PA9	Dog	Female	10	2019	Throat	Aichi	2.07 ± 0.32	Low	A—2	B—3	Detected	Cluster 2 (LC768011)	Cluster 1 (LC769576)
PA12	Dog	Male	16	2019	Pus	Tokyo	4.79 ± 2.97	Low	A—1	B—3	Detected	Cluster 1 (LC768012)	Cluster 1 (LC769577)
PA18	Dog	Female	8	2019	Nasal discharge	Kanagawa	44.81 ± 7.59	***High***	A—2	B—3	Detected	Cluster 1 (LC768013)	Cluster 1 (LC769578)
PA23	Cat	Female	15	2019	Pus	Chiba	7.50 ± 4.45	Low	A—2	B—1	Detected	Cluster 1 (LC768014)	Cluster 1 (LC769579)
PA30	Dog	Female	11	2019	Nasal discharge	Saitama	17.47 ± 8.75	***High***	A—2	B—3	Detected	Cluster 2 (LC768015)	Cluster 3 (LC769580)
PA33	Dog	Female	15	2019	Nasal discharge	Chiba	0.69 ± 0.26	Low	A—2	B—3	Detected	Cluster 2 (LC768016)	Cluster 2 (LC769581)
PA38	Dog	Female	12	2019	Postnasal discharge	Chiba	1.19 ± 0.61	Low	A—1	B—2	Detected	Cluster 1 (LC768017)	Cluster 3 (LC769582)
PA42	Dog	Male	Unknown	2021	Blood	Okayama	16.86 ± 2.98	***High***	A—2	B—3	Detected	Cluster 2 (BPUX01000001.1)	Cluster 3 (BPUX01000012.1)
PA43	Dog	Male	11	2021	Pus	Saitama	0.93 ± 0.49	Low	A—1	B—3	Detected	Cluster 2 (LC768018)	Cluster 1 (LC769583)
PA44	Dog	Female	Unknown	2021	Pus	Nagasaki	35.65 ± 15.88	***High***	A—1	B—2	Detected	Cluster 1 (LC768019)	Cluster 2 (LC769584)
PA46	Dog	Male	14	2021	Nasal discharge	Tokyo	0.81 ± 0.12	Low	A—2	B—3	Detected	Cluster 2 (LC768020)	Cluster 1 (LC769585)
PA47	Dog	Male	14	2021	Ear discharge	Chiba	38.79 ± 15.77	***High***	A—2	B—3	Detected	Cluster 1 (LC768021)	Cluster 1 (LC769586)
PA75	Dog	Female	14	2021	Nasal discharge	Tokyo	0.98 ± 0.59	Low	A—2	B—3	Detected	Cluster 1 (LC768032)	Cluster 2 (LC769597)
PA76	Dog	Male	7	2021	External naris	Tokyo	17.27 ± 7.10	***High***	A—1	B—3	Detected	Cluster 2 (LC768033)	Cluster 1 (LC769598)
PA77	Dog	Female	13	2021	Pus	Tokyo	35.78 ± 5.65	***High***	A—2	B—3	Detected	Cluster 1 (LC768034)	Cluster 2 (LC769599)
PA79	Dog	Female	13	2021	Skin	Chiba	1.14 ± 0.45	Low	A—1	B—3	Detected	Cluster 1 (LC768036)*	Cluster 3 (LC769601)
PA80	Dog	Female	2	2021	Pus	Tokyo	2.38 ± 0.22	Low	A—2	B—3	Detected	Cluster 1 (LC768037)	Cluster 1 (LC769602)
PA48	Human	Male	73	1998	Pus	Tokyo	1.79 ± 0.31	Low	A—2	B—1	Detected	Cluster 1 (LC768022)	Cluster 1 (LC769587)
PA49	Human	Male	67	2017	Sputum	Chiba	0.08 ± 0.07	Low	A—1	B—2	Detected	Cluster 1 (LC768023)	Cluster 2 (LC769588)
PA50	Human	Female	12	2017	Pus	Chiba	0.59 ± 0.30	Low	A—1	B—3	Detected	Cluster 2 (LC768024)	Cluster 1 (LC769589)
PA51	Human	Male	59	2017	Pus	Chiba	3.55 ± 1.29	Low	A—2	B—1	Detected	Cluster 1 (LC768025)	Cluster 2 (LC769590)
PA52	Human	Female	68	2018	Pus	Chiba	24.75 ± 5.43	***High***	A—1	B—3	Detected	Cluster 2 (LC768026)	Cluster 3 (LC769591)
PA53	Human	Male	80	2018	Sputum	Chiba	29.94 ± 9.46	***High***	A—2	B—3	Detected	Cluster 2 (LC768027)	Cluster 1 (LC769592)
PA54	Human	Female	10	2019	Pus	Chiba	7.21 ± 1.28	Low	A—2	B—3	Detected	Cluster 1 (LC768028)	Cluster 1 (LC769593)
PA55	Human	Male	56	2019	Sputum	Chiba	2.66 ± 1.04	Low	A—2	B—1	Detected	Cluster 2 (LC768029)	Cluster 1 (LC769594)
PA56	Human	Female	19	2019	Pus	Chiba	4.79 ± 1.45	Low	A—2	B—3	Detected	Cluster 1 (LC768030)	Cluster 1 (LC769595)
PA57	Human	Male	68	2021	Pus	Saitama	0.41 ± 0.15	Low	A—2	B—3	Detected	Cluster 2 (BQFX01000012.1)	Cluster 1 (BQFX01000001.1)
PA64	Human	Female	3	2019	Pus	Chiba	4.57 ± 1.84	Low	A—1	B—3	Detected	Cluster 2 (LC768031)	Cluster 2 (LC769596)
PA78	Human	Unknown	Unknown	1997	Pus	Tokyo	2.33 ± 0.41	Low	A—1	B—3	Detected	Cluster 1 (LC768035)	Cluster 2 (LC769600)
PA81	Human	Female	63	2017	Pus	Gifu	1.79 ± 0.55	Low	A—2	B—1	Detected	Cluster 1 (LC768038)	Cluster 1 (LC769603)

CFU, colony forming units; SD, standard deviation; RAPD, randomly amplified polymorphic DNA; *tadD*, tight adherence protein D gene; *ptfA*, type IV fimbriae gene; *ompA*, outer membrane protein A gene.
We placed the companion animal-origin (n = 17) and human-origin (n = 13) isolates in the upper and lower portions, respectively. Gray shading shows whole-genome sequences and their related features of *P. canis* isolates.
We designated CIA values higher than mean (10.45 CFU/100 cells) of all isolates as high-frequency and CIA values lower than the mean as low-frequency. High-frequency CIA are shown in bold and italic letters.
We found high percent identities of *tadD* nucleotide/amino acid (minimum 97.82%/98.99%) of the twenty-seven isolates (except for the three isolates PA52/PA54/PA55).
* *ptfA* genotype of PA79 had an inserted guanine and possessed a stop codon within coding DNA sequence. *ptfA* and *ompA* genotypes of National Collection of Type Cultures 11621(T) belonged to clusters 1 and 3, respectively.

DMEM supplemented with 10% fetal bovine serum. After 2 hr of incubation at 37 °C, the cells were washed with phosphate-buffered saline to remove the extracellular bacteria. The monolayers were maintained in media containing gentamicin (50 μg/mL)[3] for 1 hr. We confirmed the gentamicin treatment enabled to eradication of the three isolates (PA42/PA57/PA78) as the preliminary data. Whole cells were trypsinized using 0.05% trypsin (containing 0.2 mmol/L EDTA) for 2 min to detach the monolayer cells from the plate, vortexed, and disrupted with sterile distilled water to obtain cell extracts. We confirmed that the trypsin treatment had no effect on the viability of the three isolates (PA42/PA57/PA78) as the preliminary data. The cell lysates were serially diluted with Dulbecco's phosphate-buffered saline without calcium and magnesium to the appropriate concentrations and plated on 5% sheep blood agar plates to determine the internalized bacterial count 3 hr after *P. canis* inoculation. The number of internalized bacterial CFU per 100 HaCaT cells was measured. Data are expressed as mean ± standard deviation of CFU/100 cells in four wells for one isolate. We designated CIA higher than the mean value of all 30 isolates as high-frequency and that lower than the mean as low-frequency.

Genotyping was conducted using RAPD-/M13-PCR fingerprinting, as previously reported[1,6,11].

Table 2. Polymerase chain reaction (PCR) assays to determine genotypic traits of thirty *P. canis* isolates from Japan.

Target element (meaning or encoding protein)	Primer name	Direction	Sequence (5'→3')	Length (mer)	Tm (°C)†	Expected amplicon size (bp)	Reference
Randomly amplified polymorphic DNA [RAPD] (repetitive sequence)	OPA-11	forward	CAATCGCCGT	10	29		2), 10)
	AP2	reverse	GTTTCGCTCC	10	25		
M13 (repetitive sequence)	M13 core	forward & reverse	GAGGGTGGCGGTTCT	15	47		6)
tadD (tight adherence protein D)	tadD_F*	forward	TCTATTGTTGGTTGTTCCGC	20	51	672	This study
	tadD_R*	reverse	TGCATTAATCAGATCATCAGGAG	23	53		
ptfA (type IV fimbriae)	ptfA-outer_F*	forward	CGTTCTTAGTCCGTTTAGCAACC	23	56	641	This study
	ptfA-outer_R*	reverse	AACGGTAAGGCAAAATAGCGC	21	55		
ompA (outer membrane protein A)	ompA-outer_F*	forward	AGAAATTCAGGCAAATTCCAGCC	23	55	1348	This study
	ompA-outer_R*	reverse	GCGACTAAGATCAATACAATCCAC	24	54		

* The same primers were used for both PCR amplification and direct sequencing.
† Melting temperature (Tm) was calculated using nearest neighbor method.
To do RAPD fingerprinting, we conducted 45 cycles consisting of denaturation at 94°C for 1 min, annealing at 37°C for 1 min, and extension at 72°C for 3 min.
To do M13 fingerprinting, we conducted 35 cycles consisting of denaturation at 93°C for 40 sec, annealing at 50°C for 1 min, and extension at 72°C for 40 sec.
To amplify *tadD*, we conducted 35 cycles consisting of denaturation at 94°C for 1 min, annealing at 52°C for 1 min, and extension at 72°C for 1 min.
To amplify *ptfA*, we conducted 35 cycles consisting of denaturation at 94°C for 1 min, annealing at 55°C for 1 min, and extension at 72°C for 1 min.
To amplify *ompA*, we conducted 30 cycles consisting of denaturation at 94°C for 1 min, annealing at 60°C for 30 sec, and extension at 72°C for 1 min.
These PCR assays were done with each isolate in duplicate or triplicate.

Table 2 lists primer sequences, melting temperatures, and reaction conditions. The RAPD-forward/reverse primers and M13 a single primer are 10/10 and 15 nucleotides, respectively. In contrast, the repetitive extragenic palindromic (REP)- and enterobacterial repetitive intergenic consensus (ERIC)-forward/reverse primers are 18/18 and 21/22 nucleotides, respectively, which we applied[8]. To obtain the diverse fingerprinting images, RAPD-/M13-primers were selected. The PCR products were examined by 1.5% agarose gel electrophoresis in Tris-acetate-EDTA buffer. Fingerprinting was performed in duplicate or triplicate. We used a *P. multocida* isolate (PA60) from the sputum of a human patient as a positive control. Based on the PCR product images, the unweighted pair group method with arithmetic mean (UPGMA) dendrograms were constructed using the Jaccard index from the RAPD-/M13-PCR fingerprinting data. We used two applications, DendroUPGMA (http://genomes.urv.cat/UPGMA/index.php) and NJplot (http://doua.prabi.fr/software/njplot). Clades were determined based on dendrogram data. The CIA results and host species were combined with the dendrogram findings.

We speculated that the *P. canis* CIA can be associated with the tight adherence proteins, pili, and outer membrane proteins and determined the VAG profiles containing *tadD–ptfA–ompA*. Table 2 lists the primer sequences, melting temperatures, reaction conditions, and expected amplicon sizes. Primer sequences were established based on the whole-genome sequences of PA42 (GenBank accession number BPUX01000000), PA57 (BQFX01000000), HL_NV12211 (CP085871.1), HL1500 (CP083396.1), and the National Collection of Type Cultures (NCTC) 11621(T) (UGTV01000000). After obtaining the complete coding DNA sequences, we conducted genotype clustering based on the constructed phylogenetic trees.

Ethical committees from the Kitasato Institute Hospital, Kitasato University Medical Center, Sanritsu Zelkova Veterinary Laboratory, Sanritsu Laboratory, and Chiba Kaihin Municipal Hospital reviewed and approved the study design to maintain human and animal privacy (approval numbers: 21061, 2021033, SZ20220525, 22-01, and 2021-02, respectively).

We performed a two-sided Fisher's exact test to analyze the significant relationships between high-frequency CIA and host species or source. The Mann–Whitney U test for nonparametric

pairwise comparison data and Kruskal–Wallis test followed by Steel–Dwass test for nonparametric multiple comparison data were conducted to analyze significant associations between clades/clusters and high-frequency CIA or host species. Statistical significance was set at $P < 0.05$.

Table 1 summarizes the CIA values and high-/low-frequencies of the 30 *P. canis* isolates. High-frequency CIA (higher than the mean of 10.45 CFU/100 cells of all isolates) was found in nine isolates, whereas low-frequency CIA in twenty-one. We observed no significant relationships between high-frequency CIA and host species (humans) or isolation source (pus/skin).

Figure 1 shows two UPGMA dendrograms based on the fingerprinting data by RAPD-/M13-PCR (A/B). *P. multocida* (PA60, positive control) was identified as an outlier in both dendrograms. There were two (A–1/A–2) and three (B–1/B–2/B–3) clades in the RAPD- and M13-based dendrograms, respectively. We found no significant associations between high-frequency CIA or human population and two (A–1/–2) clades on the RAPD-dendrogram or three (B–1/–2/–3) clades on the M13-dendrogram.

Table 1 shows the VAG profiles (*tadD–ptfA–ompA*) of each isolate. We found high percent identities of *tadD* nucleotide/amino acid (minimum 97.82%/98.99%) of the twenty-seven isolates (except for the three isolates PA52/PA54/PA55), suggesting a low possibility of *tadD* alleles. Figure 2 shows the two clusters of *ptfA* and *ompA* alleles (A and B). HL_NV12211 belonged to Clusters 2 and 3, HL1500 belonged to Clusters 1 and 2, and NCTC 11621(T) belonged to Clusters 1 and 3. There were two (1/2) and three (1/2/3) clusters in the *ptfA* and *ompA* allele-based phylogenetic trees, respectively. We found no significant associations between high-frequency CIA or human population and two (1/2) clusters in *ptfA*-phylogenetic tree or three (1/2/3) clusters in *ompA*-phylogenetic tree.

We performed the RAPD-/M13-fingerprinting techniques, because the multilocus sequence typing (MLST) is not established for *P. canis* isolates. The REP-/ERIC- fingerprinting approaches[13,14] are carried out for molecular genotyping of enterobacteria like *Escherichia coli*. On the other hand, the RAPD-/M13-fingerprinting techniques can be used for the genotyping of broad species, such as Gram-positive pathogens (*Staphylococcus* and *Streptococcus*) and anaerobes (*Bacteroides fragilis* group and *Porphyromonas*). We found two (A–1/A–2) and three (B–1/B–2/B–3) clades in the RAPD-/M13-fingerprinting dendrograms in this investigation, whereas there were two (A–1/A–2) and three (B–1/B–2/B–3) clades in the REP-/ERIC-fingerprinting dendrograms in another study[8]. Therefore, we further should establish the MLST for molecular epidemiology of *P. canis* isolates.

Unfortunately, there were no associations between high-frequency CIA and humans (host species) or pus/skin (isolation source). We collected limited host demographics (host species–isolation source–collection year–source prefecture) of the isolates. More detailed information (underlying situations–clinical diagnosis of infections–therapeutic approaches including antimicrobial administration/surgical interventions–outcomes) should be retrieved to determine the relationship between high-frequency CIA and its clinical implications/pathogenetic significance.

Hence, our observations suggest the feasibility of CIA assessment using HaCaT cells, without relating CIA to host information or genotypic traits, by repetitive element-based fingerprinting and VAG profiling (*tadD–ptfA–ompA*). To the best of our knowledge, this is the first preliminary report of CIA assessment in human keratinocytes and genotypic traits. Further investigation of CIA in clinical isolates is needed because of a small number of isolates that we examined. We have previously reported the prevalence of unique cytolethal distending toxin genes in *P. canis* from animals and humans[18]. We observed the high percent identities of *tadD* nucleotide/amino acid and a low possibility of *tadD* alleles. Therefore, we performed only two *ptfA–ompA* allele typing. Future studies monitoring variations in VAG profiles (*ptfA–ompA* and other novel genes) using a large number of isolates are required, and we should find out relating CIA to genotypic traits.

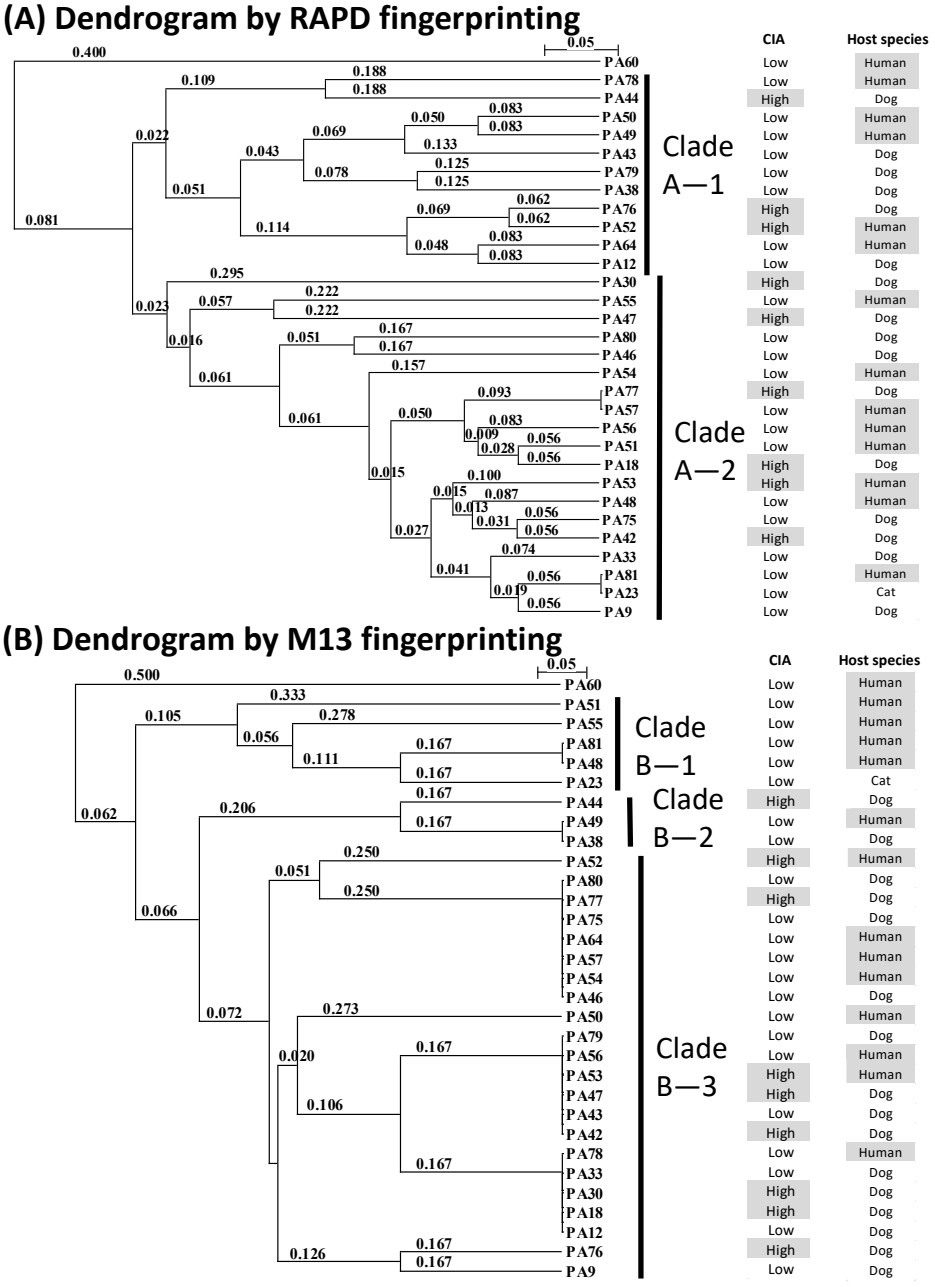

Fig. 1. The unweighted Pair Group Method with Arithmetic mean (UPGMA) dendrograms with thirty *P. canis* isolates were constructed based on the Jaccard index from fingerprinting date using polymerase chain reaction primers by randomly amplified polymorphic DNA (RAPD) sequences (A) and single primer by M13 core sequence (B). We contained a *P. multocida* isolate (PA60) from the sputum of a human patient as a positive control. We used two applications, DendroUPGMA (http://genomes.urv.cat/UPGMA/index.php) and NJplot (http://doua.prabi.fr/software/njplot). High-/low-frequencies cell invasion ability (CIA) or host species (humans/companion animals) are shown at the right-side of each isolate. PA60 revealed low-frequency CIA. Gray shading indicates the high-frequency or human isolates.

Funding Statement

This work was supported in part by the General Research Fund (2020–2022) from Graduate School of Infection Control Sciences and Ōmura Satoshi Memorial Institute.

Acknowledgments

The authors wish to thank Mr. Goro Kurita DVM (Laboratory of Infectious Diseases, Graduate School of Infection Control Sciences, Kitasato University, Tokyo, Japan) for his useful

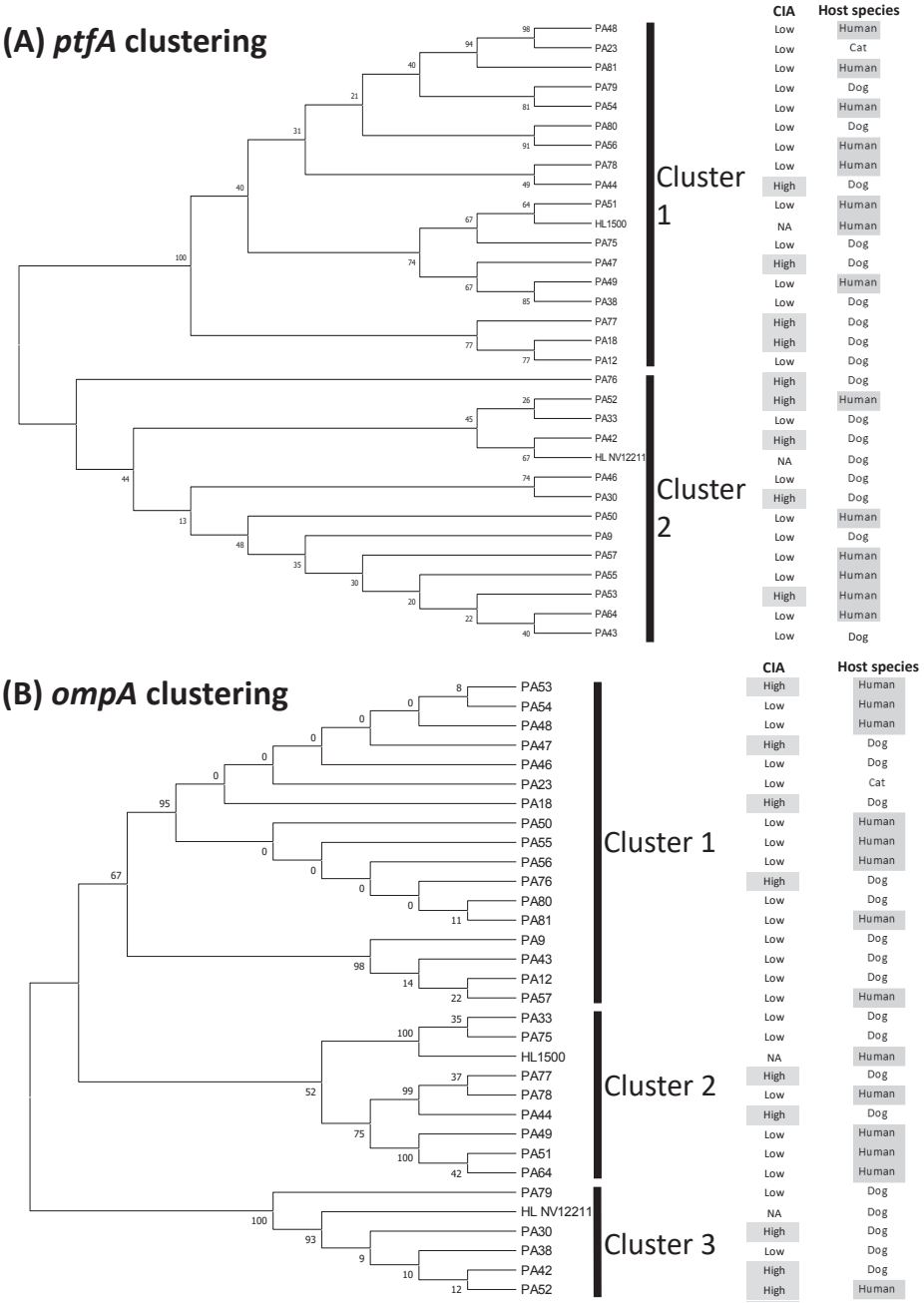

Fig. 2. Phylogenetic trees using the Neighbor-Joining method and maximum likelihood method with Whelan and Goldman model were constructed based on *ptfA* nucleotide sequences (A) and *ompA* amino acid sequences (B), respectively. High-/low-frequencies cell invasion ability (CIA) or host species (humans/companion animals) are shown at the right-side of each isolate. Gray shading indicates the high-frequency or human isolates. NA, not available.

discussions and suggestions and Editage (http://www.editage.jp) for its English proofreading.

Conflict of Interest Statement

None to declare.

References

1) Dziva F, Christensen H, Olsen JE, Mohan K. Random amplification of polymorphic DNA and phenotypic typing of Zimbabwean isolates of *Pasteurella multocida*. Vet Microbiol 82, 361–372, 2001. doi: 10.1016/s0378-

1135(01)00406-0.
2) Ferreira TSP, Moreno LZ, Felizardo MR, de Gobbi DDS, Filsner PHNL, de Moura Gomes VT, Moreno M, Moreno AM. Pheno- and genotypic characterization of *Pasteurella multocida* isolated from cats, dogs and rabbits from Brazil. Comp Immunol Microbiol Infect Dis 45, 48–52, 2016. doi: 10.1016/j.cimid.2016.02.004.
3) Galdiero M, De Martino L, Pagnini U, Pisciotta MG, Galdiero E. Interactions between bovine endothelial cells and *Pasteurella multocida*: association and invasion. Res Microbiol 152, 57–65, 2001. doi: 10.1016/s0923-2508(00)01168-2.
4) Gautier A-L, Dubois D, Escande F, Avril J-L, Trieu-Cuot P, Gaillot O. Rapid and accurate identification of human isolates of *Pasteurella* and related species by sequencing the *sodA* gene. J Clin Microbiol 43, 2307–2314, 2005. doi: 10.1128/JCM.43.5.2307-2314.2005.
5) Greco R, De Martino L, Donnarumma G, Conte MP, Seganti L, Valenti P. Invasion of cultured human cells by *Streptococcus pyogenes*. Res Microbiol 146, 551–560, 1995. doi: 10.1016/0923-2508(96)80561-4.
6) Hunt Gerardo S, Citron DM, Claros MC, Fernandez HT, Goldstein EJC. *Pasteurella multocida* subsp. *multocida* and *P. multocida* subsp. *septica* differentiation by PCR fingerprinting and α-glucosidase activity. J Clin Microbiol 39, 2558–2564, 2001. doi: 10.1128/JCM.39.7.2558-2564.2001.
7) Katoch S, Sharma M, Patil RD, Kumar S, Verma S. In vitro and in vivo pathogenicity studies of *Pasteurella multocida* strains harbouring different *ompA*. Vet Res Commun 38, 183–191, 2014. doi: 10.1007/s11259-014-9601-6.
8) Maeda T, Goto M, Tsuyuki Y, Shibata S, Shizuno K, Yoshida H, Kim J-S, Takahashi T. Biotypic and genotypic diversity in *Pasteurella canis* isolated from host animals and humans: differences in trehalose fermentation and nucleotide sequences encoding trehalose-6-phosphate hydrolase (*treC*). J Vet Med Sci 85, 858–866, 2023. doi: 10.1292/jvms.23-0165.
9) Maeda T, Yoshida H, Kim J-M, Tsuyuki Y, Kurita G, Kim J-S, Takahashi T. Draft genome sequence of blood-origin *Pasteurella canis* strain PA42, isolated from a dog in Japan. Microbiol Resour Announc 11, e00260-22, 2022. doi: 10.1128/mra.00260-22.
10) Mutters R, Ihm P, Pohl S, Frederiksen W, Mannheim W. Reclassification of the genus *Pasteurella* Trevisan 1887 on the basis of deoxyribonucleic acid homology, with proposals for the new species *Pasteurella dagmatis*, *Pasteurella canis*, *Pasteurella stomatis*, *Pasteurella anatis*, and *Pasteurella langaa*. Int J Syst Bacteriol 35, 309–322, 1985. doi: 10.1099/00207713-35-3-309.
11) Shirzad-Aski H, Tabatabaei M. Molecular characterization of *Pasteurella multocida* isolates obtained from poultry, ruminant, cats and dogs using RAPD and REP-PCR analysis. Mol Biol Res Commun 5, 123–132, 2016. doi: 10.22099/MBRC.2016.3709.
12) Shivachandra SB, Kumar A, Yogisharadhya R, Ramakrishnan MA, Viswas KN. Carboxyl terminus heterogeneity of type IV fimbrial subunit protein of *Pasteurella multocida* isolates. Vet Res Commun 37, 269–275, 2013. doi: 10.1007/s11259-013-9569-7.
13) Shivachandra SB, Kumar AA, Chaudhuri P. Molecular characterization of avian strains of *Pasteurella multocida* serogroup-A:1 based on amplification of repetitive regions by PCR. Comp Immunol Microbiol Infect Dis 31, 47–62, 2008. doi: 10.1016/j.cimid.2007.04.001.
14) Stahel ABJ, Hoop RK, Kuhnert P, Korczak BM. Phenotypic and genetic characterization of *Pasteurella multocida* and related isolates from rabbits in Switzerland. J Vet Diagn Invest 21, 793–802, 2009. doi: 10.1177/104063870902100605.
15) Talan DA, Citron DM, Abrahamian FM, Moran GJ, Goldstein EJC. Bacteriologic analysis of infected dog and cat bites. N Engl J Med 340, 85–92, 1999. doi: 10.1056/NEJM199901143400202.
16) Yoshida H, Goto M, Fukushima Y, Maeda T, Tsuyuki Y, Takahashi T. Intracellular invasion ability and associated microbiological

characteristics of *Streptococcus canis* in isolates from Japan. Jpn J Infect Dis 74, 129–136, 2021. doi: 10.7883/yoken.JJID.2020.382.
17) Yoshida H, Goto M, Maeda T, Fukushima Y, Fujita T, Tsuyuki Y, Takahashi T. Intracellular invasion ability of *Streptococcus agalactiae* among non-invasive isolates from human adults and companion animals in Japan. J Infect Chemother 27, 999–1004, 2021. doi: 10.1016/j.jiac.2021.02.017.
18) Yoshida H, Kim J-M, Maeda T, Goto M, Tsuyuki Y, Shibata S, Shizuno K, Okuzumi K, Kim J-S, Takahashi T. Virulence-associated genome sequences of *Pasteurella canis* and unique toxin gene prevalence of *P. canis* and *Pasteurella multocida* isolated from humans and companion animals. Ann Lab Med 43, 263–272, 2023. doi: 10.3343/alm.2023.43.3.263.